Neurochemistry International 62 (2013) 719–730

Contents lists available at SciVerse ScienceDirect

Neurochemistry International

journal homepage: www.elsevier.com/locate/nci

Gene profiling identifies commonalities in neuronal pathways in excitotoxicity: Evidence favouring cell cycle re-activation in concert with oxidative stress

Minghui Jessica Chen [a,1], Jian Ming Jeremy Ng [a,1], Zhao Feng Peng [b], Jayapal Manikandan [c,d], Yann Wan Yap [f], Roxana M. Llanos [f], Philip M. Beart [e,*], Nam Sang Cheung [f,*]

[a] Menzies Research Institute, University of Tasmania, Hobart, Tasmania 7000, Australia
[b] Department of Biological Science and Technology, School of Environmental Studies, China University of Geosciences, Wuhan 430074, PR China
[c] School of Anatomy, Physiology and Human Biology, The University of Western Australia, M309, 35 Stirling Highway, Crawley, WA 6009, Australia
[d] Center of Excellence in Genomic Medicine Research (CEGMR), King Fahad Medical Research Center, King AbdulAziz University, Jeddah 21589, Saudi Arabia
[e] Florey Neuroscience Institutes and Department of Pharmacology, University of Melbourne, Victoria 3010, Australia
[f] Centre for Cellular and Molecular Biology, School of Life and Environmental Sciences, Deakin University, Burwood, Victoria 3125, Australia

ARTICLE INFO

Article history:
Available online 3 January 2013

Keywords:
Excitotoxicity
Ionotropic
L-Glutamate
Ischemic stroke
Cell cycle re-activation
Neuronal death
Microarray

ABSTRACT

Excitotoxicity, induced by the aberrant rise in cytosolic Ca^{2+} level, is a major neuropathological process in numerous neurodegenerative disorders. It is triggered when extracellular glutamate (Glu) concentration reaches neuropathological levels resulting in dysregulation and hyper-activation of ionotropic glutamate receptor subtype (iGluRs). Even though all three members of the iGluRs, namely *N*-methyl-D-aspartate (NMDAR), α-amino-3-hydroxy-5-methyl-4-isoxazolepropionic acid (AMPAR) and kainate (KAR) receptors are implicated in excitotoxicity, their individual contributions to downstream signaling transduction have not been explored. In this study, we report a comprehensive description of the recruitment of cellular processes in neurons upon iGluR activation during excitotoxicity through temporal (5 h, 15 h, and 24 h) global gene profiling of AMPA, KA, NMDA, and Glu excitotoxic models. DNA microarray analyses of mouse primary cortical neurons treated with these four pharmacological agonists are further validated via real-time PCR. Bi-model analyses against Glu model demonstrate that NMDARs and KARs play a more pivotal role in Glu-mediated excitotoxicity, with a higher degree of global gene profiling overlaps, as compared to that of AMPARs. Comparison of global transcriptomic profiles reveals aberrant calcium ion binding and homeostasis, organellar (lysosomal and endoplasmic reticulum) stress, oxidative stress, cell cycle re-entry and activation of cell death processes as the main pathways that are significantly modulated across all excitotoxicity models. Singular profile analyses demonstrate substantial transcriptional regulation of numerous cell cycle proteins. For the first time, we show that iGluR activation forms the basis of cell cycle re-activation, and together with oxidative stress fulfill the "two-hit" hypothesis that accelerates neurodegeneration.

1. Introduction

L-Glutamate (Glu) is the most abundant excitatory neurotransmitter in the central nervous system (CNS) and is the only physiological agonist activating for glutamate receptors (GluRs) in the mammalian brain. GluRs play important roles in structuring neurocognitive processes underlying memory and learning (Mukherjee and Manahan-Vaughan, 2013). Therefore, when the regulation of GluR activation is impaired, not only its signaling properties are affected, but the consequences can also lead to cell death via excitotoxicity. Excitotoxicity is a general term that defines a damage-inflicting cellular process mediated via overstimulation of GluRs to effect a rise in cytosolic calcium ion level (Arundine and Tymianski, 2003). Because cellular indices reflecting excitotoxic damage are altered early in the pathogenesis of various neurodegenerative diseases such as Alzheimer's disease (AD; (Hynd et al., 2004)), dementia associated with Down syndrome (DS; (Scheuer et al., 1996)) and acute neurological deficits due to traumatic brain injury (TBI) and stroke (Arundine and Tymianski, 2004), excitotoxicity, is believed to be one of the primary upstream events that induces neuronal injury at a cellular level.

Depending on their individual mode of activation, GluR are grouped into either metabotropic (mGluRs) or ionotropic (iGluRs) GluRs (Niciu et al., 2012). While mGluRs indirectly activate ion channel via signaling pathways that involve G proteins, iGluRs possess intrinsic ion channel activities. Therefore, during

* Corresponding authors. Tel.: +61 3 92446100 (N.S. Cheung).
E-mail address: steve.cheung@deakin.edu.au (N.S. Cheung).
[1] These authors contributed equally to this study.

0197-0186/$ - see front matter © 2013 Elsevier Ltd. All rights reserved.
http://dx.doi.org/10.1016/j.neuint.2012.12.015

excitotoxicity, neuronal cell death is mediated by two concurrent yet distinct signaling processes determined by both iGluRs and mGluRs (Lea and Faden, 2003). In particular, iGluRs are made up of *N*-methyl-D-aspartate (NMDA), α-amino-3-hydroxy-5-methyl-4-isoxazolepropionic acid (AMPA) and kainate (KA) receptor subtypes which are named after their specific pharmacological agonists active at different intrinsic ligand-gated ion channel activity that allows passage of Na^+ and Ca^{2+} ions through a pore. All three subtypes of iGluRs (NMDAR, AMPAR and KAR) are actively involved during excitotoxic neuronal cell death. The NMDAR plays a major role due to its abundant expression and highest Ca^{2+} permeability (Hara and Snyder, 2007). Studies have shown that excessive NMDAR activation induces Ca^{2+} influx and release from intracellular stores, resulting in the activation of cytoplasmic proteases such as calcium-activated calpains (Simpkins et al., 2003) that hydrolyze cytoskeletal proteins. An example of such cytoskeletal protein is α-fodrin (Posner et al., 1995; Siman et al., 1989). Furthermore, NMDAR activation can result in the destabilization of lysosomes and the release of lysosomal cathepsins, causing cell death (Graber et al., 2004; Tenneti et al., 1998). Likewise, dysregulation of AMPAR and KAR also induces excitotoxicity in neurons (Jayakar and Dikshit, 2004; Sattler and Tymianski, 2001; Vincent and Mulle, 2009). Indeed, we were the first to demonstrate that AMPA alone could produce apoptotic-like injury (Larm et al., 1997), just as can KA, with injury likely to exert an apoptotic-necrotic continuum of programmed cell death (Cheung et al., 1998).

To date, the consequences of activation of individual iGluRs subtypes in downstream signal transduction during excitotoxicity has not been comprehensively and simultaneously explored in a comparative platform, impeding an understanding of the relative contributions of individual iGluRs, be that via convergent or divergent cellular pathways, towards excitotoxic damage. In our current study, global transcriptomic profiling was employed to elucidate downstream signaling pathways, in terms of amplification and diversification, subsequent to different iGluR activation to model the sequence of events subsequent to extracellular Glu in the brain reaching pathological concentrations. Here, the DNA microarray technique was applied to four excitotoxic models induced by (a) the general GluR agonist, Glu, (b) AMPAR agonist, AMPA, (c) NMDAR agonist, NMDA and (d) KAR agonist, KA. Subsequent comparative global gene profile analysis was performed to elucidate the major primary biological processes regulated by iGluRs in the trigger of excitotoxicity during Glu-mediated neuronal injury. Our study is the first to attempt global gene profiling of this type and scale to elucidate the pathobiology of excitotoxicity. Briefly, oxidative stress and cell cycle re-activation were identified as the primary cellular pathways that were significantly modulated. The specific association of cell cycle-reactivation with iGluR activation provided interesting evidence for the occurrence of a 'two-hit' hypothesis in excitotoxicity that has been previously postulated by others for the basis of neurodegeneration in AD pathogenesis (Zhu et al., 2004, 2007).

2. Materials and methods

2.1. Murine neocortical neuronal cultures

Neocortical neurons (gestational days 15 or 16) obtained from foetal cortices of Swiss albino mice were used to prepare the primary cultures as previous described with minor modifications (Cheung et al., 2000). Dissected cortices were subjected to trypsin digestion and mechanical trituration. Cells were collected by centrifugation and resuspended in Neurobasal™ (NB) medium containing 2.5% B27 supplement, 1% penicillin, 1% streptomycin, 0.25% GlutaMAX-1 supplement, and 10% dialyzed foetal calf serum. 24-Well plates previously coated with poly-D-lysine (100 μg/ml) were seeded with cells to a density of 2×10^5 cells/cm^2 and used for subsequent experiments. Cultures were maintained in a humidified 5% CO_2 and 95% air incubator at 37 °C. Immunocytochemical staining of the cultures at day 5 *in vitro* for microtubule-associated protein-2 and glial fibrillary acidic protein revealed >95% of the cells were neurons with minimal contamination by glia (Cheung et al., 1998). All experiments involving animals were approved by the National University of Singapore, and were in accordance with the US Public Health Service guide for the care and use of laboratory animals.

2.2. Drug preparation and treatment

Glu, NMDA, KA and *S*-AMPA (Sigma–Aldrich) were freshly prepared prior to usage to achieve stock concentrations of 100 mM. Working concentrations (Glu 250 μM, NMDA 200 μM, KA 100 μM and *S*-AMPA 300 μM) were achieved by dilution with NB medium.

2.3. Total RNA extraction and isolation

RNA was extracted using RNeasy Mini Kit (Qiagen Cat. No. 74104) according to the manufacturer's instructions. All pipette tips used were RNase-free. Each sample was prepared from 1×10^6 cultured cells. RNA concentration was determined spectrophotometrically using Nanodrop ND-1000 Version 3.2.1 and RNA quality was determined using a E-gene HDA-GT12 genetic analyzer.

2.4. Microarray analysis using Illumina Mouse Ref8 Ver.1.1 hybridization beadchips

Microarray was carried out using Illumina® Mouse Ref8 Ver.1.1 arrays. For each GluR agonist treatment, the assignment of the arrays was as follow: 5 h ($n = 3$), 15 h ($n = 3$), and 24 h ($n = 3$) and control ($n = 6$). Each RNA sample (500 ng) was reverse transcribed using T7 Oligo(dT) primer to form first strand cDNA containing a T7 promoter sequence, which was subsequently used for the second strand cDNA synthesis (employing DNA polymerase and Rnase H to simultaneously degrade the RNA and to synthesize second strand cDNA). The cDNAs were purified to remove RNA, primers, enzymes, and salts that would inhibit *in vitro* transcription. Finally *in vitro* transcription was employed to generate multiple copies of biotinylated cRNA from the double-stranded cDNA templates. All previously mentioned procedures were performed using Illumina® TotalPrep RNA Amplification Kit. cRNA yields were quantitated using the NanoDrop ND-1000.

cRNA (750 ng) prepared in RNase-free water (5 μl) was mixed with hybridization buffer (10 μl) and preheated to 65 °C for 5 min. Assay samples were then fully loaded onto the large sample port of each array on the beadchip. Beadchips were incubated in a humidified hybridization chamber at 58 °C for 17 h. The following day, the IntelliHyb seal on the beadchip was removed to expose all the arrays. Beadchips were blocked and labeled with streptavidin-Cy3, followed by stringency buffer washes and dried. The hybridization process was carried out according to the manufacturer's instruction (Illumina Inc.). Beadchips were then ready for scanning on the Illumina® scanner using Bead Studio software at Scan Factor = 0.8.

2.5. Microarray data collection and analysis

Initial analysis of the scanned images was performed using BeadScan (Illumina). The absolute data (signal intensity, detection call and detection *p*-value) were exported into GeneSpringGX 7.3 (Agilent Technologies, CA, USA) software for analysis by a paramet-

ric test based on crossgene error model (PCGEM). A one-way analysis of variance (ANOVA) approach was used to identify differentially expressed genes. Array data were globally normalized using GeneSpring software. Firstly, all measurements on each chip were divided by the 50th percentile value (per chip normalization). Secondly, each gene was normalized to the baseline value of the control samples (per gene normalization) using median. Then genes were filtered on fold change ±1.5-fold against controls in at least one of three conditions for each respective treatment. Finally, one-way ANOVA ($p < 0.05$) and Benjamini–Hochberg false discovery rate (FDR) Correction were used to seek differentially expressed genes. Genes which were differentially expressed are annotated according to gene ontology-biological process provided by the online bioinformatics resources Database for Annotation, Visualization and Integrated Discovery (DAVID) 6.7 (http://david.abcc.ncifcrf.gov/) (Dennis et al., 2003; Huang et al., 2009). All microarray data reported here are described in accordance with MIAME guidelines, and has been deposited in the NCBIs Gene Expression Omnibus (GEO; http://www.ncbi.nlm.nih.gov/geo/) and are accessible through GEO Series accession number GSE16035, GSE22993, GSE22994 and GSE19936.

2.6. Real-time polymerase chain reaction (PCR)

Eight differentially expressed genes were selected for validation of the microarray results by quantitative real-time PCR. Microarray biological triplicates were combined into one sample for subsequent analysis in duplicate per probe. The same total RNAs used for microarray from mouse culture treated with 250 μM Glu were reverse transcribed to cDNAs according to steps specified by the manufacturer (Applied Biosystems Taqman reverse transcription reagents). The experiment set up, briefly, consisted of Taqman master mix (20 μl) and cDNA or water (NTC; both 5 μl) was added to the designated reaction well of a real-time PCR plate. The plate was then read using the 7000 Fast Real-Time PCR System with conditions according to the manufacturer's protocol.

3. Results

Overall, cellular transcriptional regulation was assessed in excitotoxic models employing 250 μM Glu, 200 μM NMDA, 300 μM AMPA and 100 μM KA over a 24-h period using Illumina® Mouse Ref8 V1.1 genechips. The raw transcriptional signal data from individual arrays were then subjected to statistical filtering using one-way ANOVA, $p < 0.05$ and Benjamini–Hochberg FDR. Gene probes were considered to be significantly regulated when they demonstrated gene expression changes of at least ±1.5 folds in a minimum of one out of the three time-points (5 h, 15 h, and 24 h). All gene probes that passed these selection criteria were gathered to form the global transcriptomic data for each excitotoxic model. Transcriptomic profiles generated from the treatment of neurons with Glu (1842 gene probes), NMDA (2309 gene probes), AMPA (1563 gene probes) and KA (3800 gene probes) were organized side-by-side and partitioned to different fold-change categories (Fig. 1). A substantial number of gene probes demonstrated greater than ±1.5-fold-changes in gene expression over the 24-h period, with KA treatment generating the largest transcriptomic profile.

3.1. Bi-model analyses of individual iGluRs profiles against that of Glu revealed the following decrease ordering of iGluRs activation dependence NMDARs>KARs>AMPARs during excitotoxicity

Bi-model global transcriptomic profile comparisons using Glu model as the basis of analysis demonstrated that in rank order of highest to lowest degree of overlap, i.e. commonly occurring and differentially regulated gene probes, NMDA > KA > AMPA (Fig. 2). NMDA (Fig. 2A) and KA (Fig. 2C) profiles were comparable, but they exhibited nearly double the number of Glu commonly occurring genes when compared to AMPA profile (Fig. 2B). These profiles signify a greater reliance upon NMDAR and KAR-mediated signaling pathways to induce excitotoxicity during Glu-mediated neurotoxicity. A more in-depth analysis of the consistency in transcriptional regulatory trend demonstrated that the majority of the genes were similarly regulated at 15 h and 24 h, respectively in all three iGluRs models (Fig. 3).

3.2. Simultaneous comparison of all four excitotoxic models identified several major common biological processes

A concerted transcriptomic analysis of all four profiles revealed a total list of 583 common genes. Similarly, a detailed exploration of the transcriptional trend of these genes revealed a high degree of consistency at each respective time-point, which faltered upon inter-time-point examination across all three time-points (Fig. 4), indicating a common temporal activation and/or inhibition of

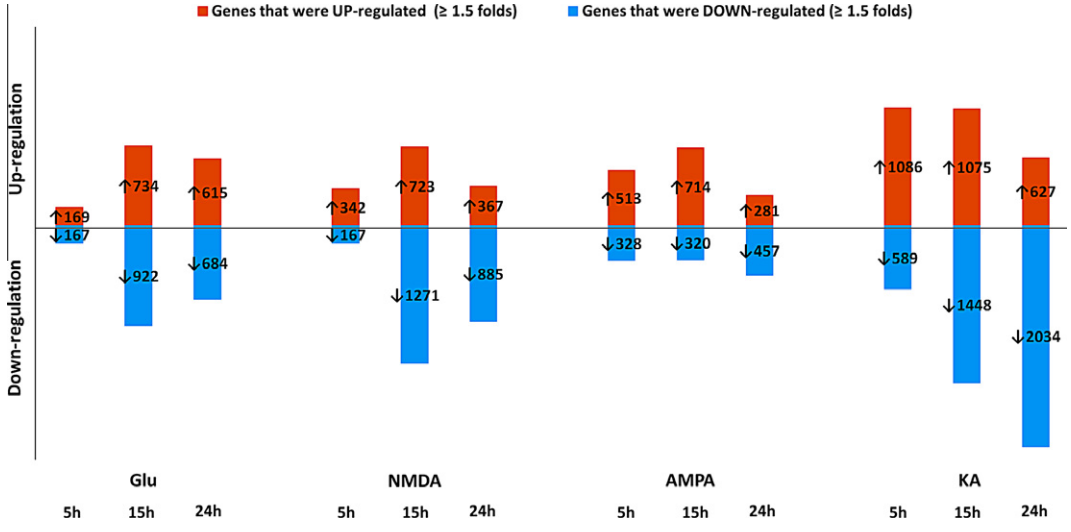

Fig. 1. Classification of individual iGluRs global transcriptomic profiles (passed microarray selection criteria: total numbers of genes showing expression at least ±1.5-fold change in a minimum of one out of the three time-points (5 h, 15 h, and 24 h) and statistical examination using one-way ANOVA, $p < 0.05$ and Benjamini–Hochberg FDR) according to specific time-points and fold-change expression up/down-regulated.

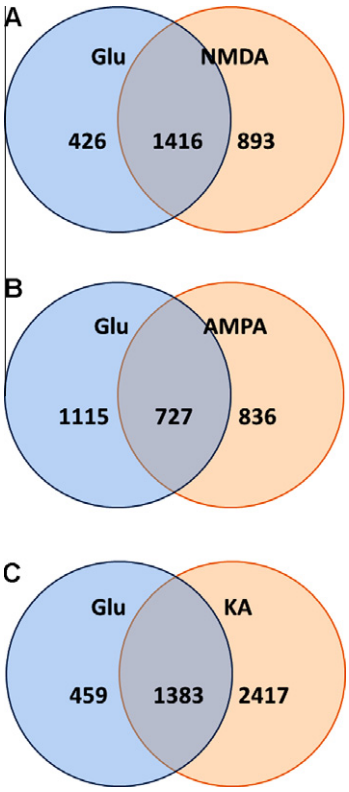

Fig. 2. Bi-model global transcriptomic profile analysis of individual iGluRs agonists against Glu excitotoxic model. Venn diagrams demonstrating the number of gene probes common and mutually exclusive to both models [A] Glu against NMDA [B] Glu against AMPA and [C] Glu against KA.

signaling pathways across all four excitotoxicity models, but with distinct progression outcome of each signaling cascade, i.e. either pursuant and persistent maintenance of initial activated/inhibitory state or directional change of pathway regulation.

Functional classification of these 583 RefSeq transcripts, which corresponded to 485 biologically-annotated genes, identified several important and over-represented biological pathways relevant to the progression of excitotoxicity (Table 1). These include calcium homeostasis and binding, anti-oxidant response, cell death and cell survival processes. Notably, an overwhelming number of molecules involved in the promotion of mitotic cell cycle progression were transcriptionally elevated in all four models of excitotoxicity. Consistently, all members of these over-represented biological processes were significantly modulated at the expression level between the 5 h and 15 h time-points, implying the reported pathways constitute the early upstream cellular events in excitotoxicity.

3.2.1. Calcium ion homeostasis and binding

In all four excitotoxic models, genes encoding for Ca^{2+}-dependent proteins and receptors (Gpr12, Prkcb and Rxfp3) were significantly down-regulated, indicating the occurrence of aberrant calcium ion homeostasis. On the contrary, genes encoding for Ca^{2+}-binding proteins (S100a6 and Anx (A2, A3, and A5) showed increased gene expression, providing further evidence of elevation of cytosolic Ca^{2+}level during excitotoxicity due to activation of iGluRs which triggers intrinsic Ca^{2+}channel activity.

3.2.2. Lysosomal stress

Aberrant elevation of cytosolic Ca^{2+} ion level and overproduction of reactive oxygen species (ROS) imposes organellar stress through disruption of the delicate balance of cellular ionic gradients and unregulated modifications of cellular proteins resulting in detrimental loss/gain-of function, all contributing to disturbance of normal cellular signaling. Analysis of the gene profiles of genes common to all four excitotoxic models revealed significant transcriptional activation of lysosomal resident proteins, indicative of some form of disorientation and/or stress imposed on the normal functioning of the lysosomes.

3.2.3. Anti-oxidant responses

3.2.3.1. Heat shock proteins (Hsps) and molecular chaperones. Organellar (ER and lysosomal) stress is especially prominent in excitotoxicity and evokes a cellular counteractive response to minimize electrophilic and oxidative burdens. Interestingly, comparative microarray analysis demonstrated that in our specific iGluR excitotoxic models, up-regulation of the majority of genes encoding for heat shock proteins (HSPs) and molecular chaperones (Hmox1, Srxn1, Hspa2, and Hspb8) and metal chaperones (Mt3) occurred at the 5 h time-point, much earlier than that of Glu at 15 h.

3.2.3.2. Glutathione (GSH) metabolism. Genes transcribing for members of the GSH anti-oxidative pathway were significantly up-regulated in all four models. However, AMPA and Glu models demonstrated significant elevation of GSH pathway genes at 15 h, while NMDARs and KARs demonstrated earlier transcriptional response at 5 h.

3.2.4. Cell death

Majority of the genes encoding for proteins directly/indirectly involved in promotion of cell death (Angptl4, Casp6 and Ctnna1) were transcriptionally up-regulated. In addition, cell death was further accelerated by the down-regulation of anti-cell death protein (Bcl11b).

3.2.5. Cell homeostasis, survival and proliferation

In all four excitotoxic models, genes encoding for pro-survival/mitogenic proteins (Spp1 and Birc5 (also known as Survivin)) and growth factors (Igf2 and Igfbp5) were up-regulated between the 5 h and 15 h time-points. These responses indicate a cellular response to suppress cell death mechanisms.

3.2.6. Mitotic cell cycle

Numerous genes encoding for cell cycle proteins that promote cell cycle re-entry were up-regulated in all four excitotoxic models between 5 h and 15 h. This observation is totally unprecedented in the context of excitotoxicity. Under physiological conditions, neurons are in the post-mitotic and differentiated state. Aberrant cell cycle re-entry has been implicated in the pathogenesis of several neurological conditions such as AD, DS, Huntington's disease, Pick's disease and stroke (Camins et al., 2008; Pelegri et al., 2008). Recent studies on AD suggested this cellular event to be a part of the neuronal death process (Lopes et al., 2009a, 2009b). p53, the main keeper of genome integrity, was significantly down-regulated (denoted as Trp53 in the table), indicating a failure in the cell cycle checkpoint system that enhances re-activation of cell cycle process.

3.3. Singular profile analysis highlights cell cycle re-activation as a prominent biological process during excitotoxicity

The majority of proteins involved in mitotic cell cycle process showed significant transcriptional modulation across all four profiles (Table 2). Gene expression of proteins promoting positive regulation of mitosis occurred between 5 h and 15 h post-treatment, providing strong evidence for the early occurrence of cell cycle re-entry upon iGluRs induction. Detailed temporal fold-expression of individual genes can be found in Supplementary Tables 1–4.

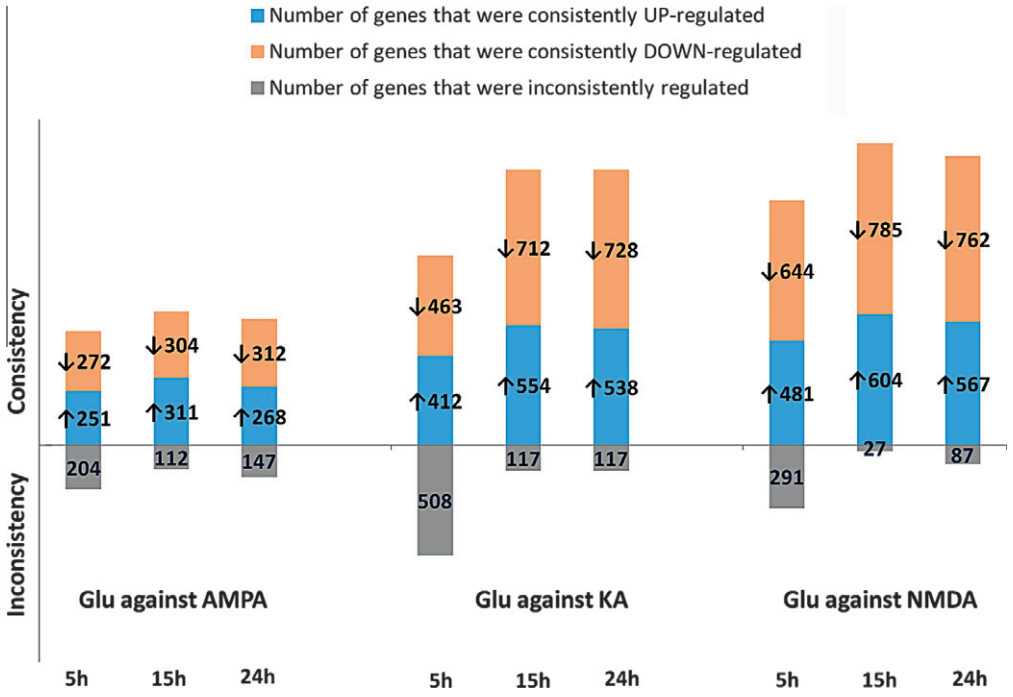

Fig. 3. Consistency in the transcriptional regulatory trend of the commonly occurring and significantly modulated gene probes in individual iGluRs against Glu excitotoxic models.

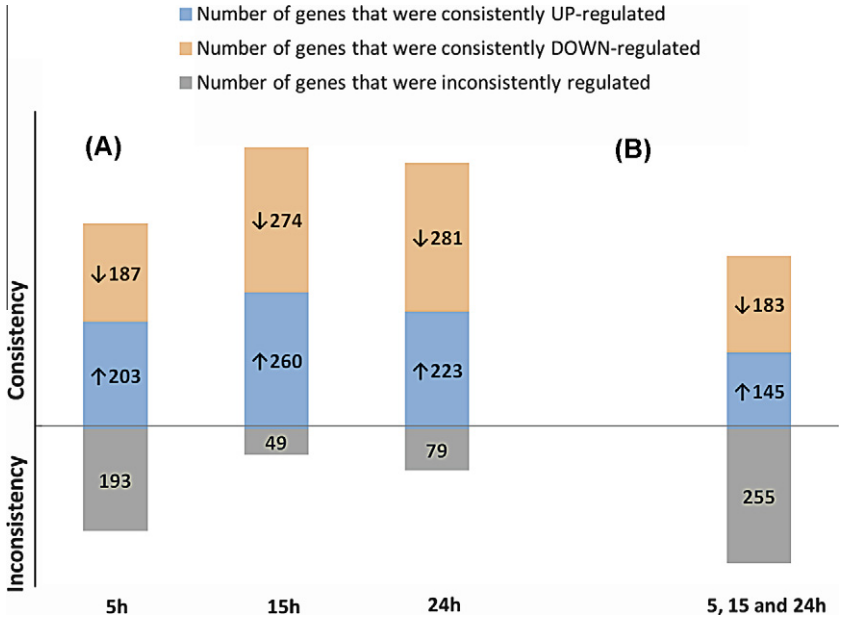

Fig. 4. Overall consistency in the transcriptional regulatory trend of the commonly occurring and significantly modulated gene probes [A] at respective time-points (5 h, 15 h, and 24 h) and [B] across all three time points in all four excitotoxic models.

3.4. Validation of Glu global transcriptomic profiles via real-time PCR

Microarray data were validated via real-time PCR using the same total RNA samples previously employed for microarray analysis. Similar temporal transcriptional regulatory trends were observed for the genes listed in Table 3.

4. Discussion

Excitotoxicity is well accepted to be a cell death process contributing to both acute and chronic neurodegenerative conditions (Doble, 1999). Although rises in intracellular Ca^{2+} subsequent to activation of NMDARs play a central role in most discussions of excitotoxicity, the recruitment of cell signaling cascades is likely to be more complex. Here, we sought to determine the individual contributions of over-stimulated iGluRs to the excitotoxic process by transcriptomic profiling. Simultaneous comparison of the global transcriptomic profiles of AMPA-, KA-, NMDA-, and Glu-mediated excitotoxic injury revealed a higher degree of correlation in terms of number of similarly-regulated genes for KA and NMDA, rather than AMPA profiles, versus that of Glu as background. The differences might be due to: (a) higher NMDAR and KAR expression on

Table 1
Gene expression profiles of neuronal death-related families in cultured mouse primary cortical neurons treated with EC_{50} concentrations of AMPA, KA, NMDA, and Glu over a 24-h period respectively. All expression values (given as fold-changes) were selected based on having at least minimum of ±1.5-fold change in at least one out of three time-points, subjected to one-way ANOVA analysis and were significant at $p < 0.05$. Values are given as mean ± SE.

Genbank	Gene title	Symbol	Time-points											
			300 μM AMPA			100 μM KA			200 μM NMDA			250 μM Glu		
			5 h	15 h	24 h	5 h	15 h	24 h	5 h	15 h	24 h	5 h	15 h	24 h
Calcium ion homeostasis and binding														
NM_008151	G-protein coupled receptor 12	Gpr12	−2.40 ± 0.09	−1.70 ± 0.15	−1.80 ± 0.14	−2.18 ± 0.13	−2.66 ± 0.12	−2.89 ± 0.11	−1.50 ± 0.19	−2.20 ± 0.11	−2.00 ± 0.13	−1.43 ± 0.19	−1.80 ± 0.17	−1.40 ± 0.18
NM_007587	Calcitonin/calcitonin-related polypeptide, alpha	Calca	1.10 ± 0.36	1.50 ± 0.47	1.20 ± 0.34	1.11 ± 0.40	2.17 ± 0.47	2.15 ± 0.67	1.10 ± 0.35	1.90 ± 0.54	1.64 ± 0.43	−1.10 ± 0.31	2.30 ± 0.66	2.80 ± 0.71
NM_008855	Protein kinase C, beta 1	Prkcb	−1.10 ± 0.21	−1.72 ± 0.16	−1.94 ± 0.12	−1.04 ± 0.27	−1.82 ± 0.12	−2.40 ± 0.12	−1.20 ± 0.26	−2.80 ± 0.09	−2.50 ± 0.09	−1.10 ± 0.23	−1.60 ± 0.12	−1.38 ± 0.18
NM_011313	S100 calcium binding protein A6 (calcyclin)	S100a6	1.17 ± 0.23	1.65 ± 0.36	1.10 ± 0.19	1.35 ± 0.24	2.12 ± 0.39	1.66 ± 0.30	1.50 ± 0.29	2.80 ± 0.51	2.22 ± 0.35	1.00 ± 0.18	1.93 ± 0.38	1.90 ± 0.37
NM_007585	Annexin A2	Anxa2	1.99 ± 0.38	1.80 ± 0.42	1.38 ± 0.31	2.30 ± 0.45	1.98 ± 0.34	1.48 ± 0.35	1.90 ± 0.38	2.24 ± 0.43	1.60 ± 0.31	1.52 ± 0.25	1.93 ± 0.31	2.05 ± 0.43
NM_013470	Annexin A3	Anxa3	1.30 ± 0.30	1.89 ± 0.48	1.66 ± 0.58	1.00 ± 0.23	1.95 ± 0.43	1.61 ± 0.42	1.50 ± 0.45	3.14 ± 0.77	2.60 ± 0.58	1.20 ± 0.31	3.60 ± 0.81	3.20 ± 0.63
NM_009673	Annexin A5	Anxa5	−1.00 ± 0.23	1.50 ± 0.31	1.10 ± 0.24	−1.00 ± 0.19	1.50 ± 0.33	1.10 ± 0.21	1.40 ± 0.27	2.00 ± 0.40	1.80 ± 0.35	1.20 ± 0.20	1.70 ± 0.29	1.60 ± 0.38
Lysosomal stress														
NM_017372	Lysozyme 2	Lyz2	1.63 ± 0.40	1.42 ± 0.36	−1.13 ± 0.24	−1.10 ± 0.29	1.50 ± 0.36	1.40 ± 0.43	1.60 ± 0.61	2.10 ± 0.69	2.10 ± 0.48	1.20 ± 0.30	1.65 ± 0.40	1.50 ± 0.44
NM_010686	Lysosomal-associated protein transmembrane 5	Laptm5	1.70 ± 0.31	1.40 ± 0.34	−1.10 ± 0.19	−1.50 ± 0.18	1.80 ± 0.34	1.40 ± 0.50	1.71 ± 0.46	2.31 ± 0.98	2.13 ± 0.34	1.34 ± 0.25	1.98 ± 0.37	1.95 ± 0.40
NM_010685	Lysosomal-associated membrane protein 2	Lamp2	1.38 ± 0.39	1.60 ± 0.41	1.30 ± 0.32	1.63 ± 0.39	2.23 ± 0.50	1.54 ± 0.37	1.44 ± 0.36	2.31 ± 0.41	1.77 ± 0.30	−1.10 ± 0.30	1.75 ± 0.51	1.70 ± 0.38
NM_019972	Sortilin 1	Sort1	1.10 ± 0.35	1.28 ± 0.50	1.22 ± 0.54	1.50 ± 0.51	2.31 ± 0.56	1.80 ± 0.46	1.50 ± 0.45	3.70 ± 0.81	2.50 ± 0.64	1.50 ± 0.45	2..00 ± 0.63	1.40 ± 0.44
NM_009906	Tripeptidyl peptidase I	Tpp1	1.20 ± 0.29	1.70 ± 0.53	1.10 ± 0.30	1.50 ± 0.40	1.95 ± 0.53	1.70 ± 0.54	1.20 ± 0.36	1.70 ± 0.40	1.30 ± 0.31	−1.10 ± 0.32	1.60 ± 0.41	1.60 ± 0.40
Anti-oxidant response – heat shock proteins and molecular chaperones														
NM_010442	Heme oxygenase (decycling) 1	Hmox1	2.32 ± 0.45	1.68 ± 0.29	1.38 ± 0.51	2.34 ± 0.39	2.17 ± 0.39	2.04 ± 0.37	2.70 ± 0.58	3.11 ± 0.48	1.60 ± 0.29	1.60 ± 0.34	2.37 ± 0.41	1.51 ± 0.38
NM_029688	Sulfiredoxin 1 homolog (S. cerevisiae)	Srxn1	2.60 ± 0.56	1.70 ± 0.34	1.30 ± 0.41	3.10 ± 0.54	1.93 ± 0.36	1.38 ± 0.30	2.00 ± 0.39	1.95 ± 0.28	1.10 ± 0.19	−1.20 ± 0.29	2.16 ± 0.73	1.17 ± 0.43
NM_007453	Peroxiredoxin 6	Prdx6	1.32 ± 0.41	1.72 ± 0.55	1.16 ± 0.37	1.10 ± 0.30	1.30 ± 0.30	1.25 ± 0.40	1.14 ± 0.36	1.62 ± 0.47	1.20 ± 0.28	−1.10 ± 0.27	2.02 ± 0.60	1.80 ± 0.56
NM_008301	Heat shock protein 2	Hspa2	1.50 ± 0.44	3.00 ± 0.76	2.30 ± 0.64	1.64 ± 0.44	2.77 ± 0.65	2.26 ± 0.64	1.00 ± 0.26	2.00 ± 0.52	2.00 ± 0.47	−1.30 ± 0.19	1.64 ± 0.36	1.60 ± 0.39
NM_030704	Heat shock protein 8	Hspb8	1.80 ± 0.45	2.20 ± 0.63	1.40 ± 0.59	1.42 ± 0.37	2.61 ± 0.59	1.60 ± 0.38	2.00 ± 0.46	3.90 ± 0.80	1.83 ± 0.46	1.29 ± 0.31	4.40 ± 1.06	2.63 ± 0.70
NM_013602	Metallothionein 1	Mt1	1.56 ± 0.28	1.74 ± 0.28	1.21 ± 0.17	2.00 ± 0.40	2.29 ± 0.38	1.92 ± 0.38	1.60 ± 0.25	2.00 ± 0.34	1.50 ± 0.24	1.10 ± 0.16	1.80 ± 0.26	1.80 ± 0.39
NM_013603	Metallothionein 3	Mt3	1.49 ± 0.26	1.80 ± 0.69	1.10 ± 0.20	2.34 ± 0.48	1.90 ± 0.34	2.00 ± 0.49	1.35 ± 0.27	1.90 ± 0.27	1.80 ± 0.55	−1.10 ± 0.17	1.60 ± 0.28	1.60 ± 0.30
Anti-oxidant response – Glutathione metabolism														
NM_010357	Glutathione S-transferase, alpha 4	Gsta4	1.10 ± 0.29	1.82 ± 0.44	1.40 ± 0.33	1.14 ± 0.31	2.30 ± 0.60	2.03 ± 0.48	1.30 ± 0.39	3.05 ± 0.70	2.14 ± 0.52	−1.20 ± 0.18	2.60 ± 0.63	2.10 ± 0.59
NM_008184	Glutathione S-transferase, mu 6	Gstm6	1.20 ± 0.40	1.50 ± 0.53	−1.00 ± 0.35	1.50 ± 0.50	1.90 ± 0.52	1.20 ± 0.36	1.45 ± 0.45	2.10 ± 0.63	1.34 ± 0.35	−1.20 ± 0.22	2.10 ± 0.58	1.70 ± 0.52
NM_019946	Microsomal glutathione S-transferase 1	Mgst1	1.10 ± 0.30	1.80 ± 0.46	1.30 ± 0.42	1.40 ± 0.44	2.55 ± 0.53	1.91 ± 0.51	1.71 ± 0.42	2.96 ± 0.60	1.67 ± 0.37	−1.00 ± 0.27	3.20 ± 0.87	2.90 ± 0.90
NM_025569	Microsomal glutathione S-transferase 3	Mgst3	−1.25 ± 0.19	−1.56 ± 0.15	−1.40 ± 0.16	−1.20 ± 0.20	−2.26 ± 0.09	−2.14 ± 0.12	−1.25 ± 0.18	−2.00 ± 0.10	−1.63 ± 0.12	−1.30 ± 0.14	−1.70 ± 0.11	−1.60 ± 0.12
NM_010358	Glutathione S-transferase, mu 1	Gstm1	1.30 ± 0.26	1.68 ± 0.27	1.10 ± 0.18	1.57 ± 0.33	2.12 ± 0.40	1.42 ± 0.40	1.45 ± 0.32	2.23 ± 0.46	1.43 ± 0.30	−1.10 ± 0.14	1.90 ± 0.37	1.64 ± 0.35
Cell death														
NM_020581	Angiopoietin-like 4	Angptl4	2.70 ± 0.59	5.32 ± 1.14	2.36 ± 0.63	4.74 ± 0.84	11.98 ± 2.14	10.21 ± 2.28	3.42 ± 0.65	7.93 ± 1.61	5.32 ± 1.00	2.00 ± 0.46	8.27 ± 1.62	8.24 ± 1.58
NM_009811	Caspase 6	Casp6	1.10 ± 0.28	1.60 ± 0.33	1.20 ± 0.32	1.30 ± 0.30	2.10 ± 0.35	1.60 ± 0.36	1.50 ± 0.39	2.42 ± 0.48	1.74 ± 0.27	1.20 ± 0.31	2.00 ± 0.37	1.70 ± 0.46
NM_009818	Catenin (cadherin associated protein), alpha 1	Ctnna1	1.30 ± ± 0.21	1.55 ± 0.24	1.20 ± 0.18	1.30 ± 0.23	2.10 ± 0.29	1.43 ± 0.27	1.55 ± 0.28	2.40 ± 0.33	1.80 ± 0.32	1.20 ± 0.20	1.90 ± 0.34	1.80 ± 0.36
NM_021399	B-cell leukemia/lymphoma 11B	Bcl11b	−1.07 ± 0.17	−1.80 ± 0.11	−1.60 ± 0.12	−1.37 ± 0.16	−1.53 ± 0.12	−1.82 ± 0.11	−1.00 ± 0.21	−2.20 ± 0.09	−1.80 ± 0.11	1.00 ± 0.17	−1.70 ± 0.10	−1.50 ± 0.12
Cell homeostasis, survival and proliferation														
NM_010835	Homeobox, msh-like 1	Msx1	1.17 ± 0.35	1.65 ± 0.48	1.00 ± 0.29	1.90 ± 0.63	2.02 ± 0.54	1.82 ± 0.46	1.25 ± 0.33	1.60 ± 0.34	1.45 ± 0.36	−1.30 ± 0.25	1.90 ± 0.57	1.80 ± 0.47

NM_152229	Nuclear receptor subfamily 2, group E, member 1	Nr2e1	1.40 ± 0.28	1.80 ± 0.38	1.30 ± 0.29	1.90 ± 0.40	2.30 ± 0.42	1.70 ± 0.35	1.40 ± 0.35	2.00 ± 0.32	1.60 ± 0.50	1.00 ± 0.21	2.00 ± 0.48	2.10 ± 0.47
NM_009263	Secreted phosphoprotein 1	Spp1	1.77 ± 0.40	1.55 ± 0.38	1.03 ± 0.28	−1.00 ± 0.32	2.43 ± 0.68	2.23 ± 0.67	1.90 ± 0.83	3.50 ± 3.20	4.30 ± 1.17	1.20 ± 0.30	2.00 ± 0.44	2.00 ± 0.45
NM_009129	Secretogranin II	Scg2	10.12 ± 2.32	11.74 ± 2.39	9.17 ± 1.77	11.00 ± 2.47	14.06 ± 2.73	12.03 ± 1.93	1.94 ± 0.44	2.44 ± 0.82	4.03 ± 0.85	1.00 ± 0.22	−4.09 ± 0.07	−3.79 ± 0.08
NM_009696	Apolipoprotein E	Apoe	1.09 ± 0.23	1.70 ± 0.29	1.30 ± 0.24	1.30 ± 0.28	2.36 ± 0.43	1.98 ± 0.36	1.15 ± 0.27	2.40 ± 0.52	1.80 ± 0.27	−1.20 ± 0.14	1.70 ± 0.32	1.70 ± 0.37
NM_009689	Baculoviral IAP repeat-containing 5	Birc5	1.94 ± 0.50	1.25 ± 0.37	−1.00 ± 0.26	2.09 ± 0.59	1.39 ± 0.35	1.21 ± 0.31	2.00 ± 0.56	1.40 ± 0.33	−1.00 ± 0.22	1.54 ± 0.36	1.88 ± 0.50	1.34 ± 0.30
NM_013863	Bcl2-associated athanogene 3	Bag3	1.80 ± 0.24	2.40 ± 0.39	2.40 ± 0.48	2.50 ± 0.37	2.49 ± 0.37	2.09 ± 0.31	2.30 ± 0.47	2.70 ± 0.36	2.50 ± 0.48	1.60 ± 0.34	2.00 ± 0.38	1.80 ± 0.45
NM_010514	Insulin-like growth factor 2	Igf2	1.40 ± 0.28	1.50 ± 0.30	1.00 ± 0.21	1.80 ± 0.35	2.10 ± 0.43	1.60 ± 0.39	1.60 ± 0.36	1.70 ± 0.41	1.30 ± 0.28	1.60 ± 0.32	2.40 ± 0.52	2.10 ± 0.52
NM_133662	Immediate early response 3	Ier3	1.40 ± 0.32	1.40 ± 0.37	1.80 ± 0.45	−1.00 ± 0.26	1.60 ± 0.31	1.60 ± 0.35	1.20 ± 0.32	1.70 ± 0.31	1.60 ± 0.27	1.90 ± 0.48	1.10 ± 0.34	1.00 ± 0.21
NM_008520	Latent transforming growth factor beta binding protein 3	Ltbp3	1.10 ± ± 0.25	1.80 ± 0.43	1.60 ± 0.32	1.05 ± 0.33	1.23 ± 0.41	1.38 ± 0.41	1.20 ± 0.26	1.60 ± 0.34	1.80 ± 0.35	−1.00 ± 0.22	1.50 ± 0.25	1.90 ± 0.41
NM_010518	Insulin-like growth factor binding protein 5	Igfbp5	−1.10 ± 0.25	1.60 ± 0.32	1.10 ± 0.26	1.30 ± ± 0.26	2.14 ± 0.38	1.61 ± ± 0.40	1.10 ± 0.25	2.00 ± 0.40	1.80 ± ± 0.39	−1.20 ± 0.12	1.70 ± 0.28	1.90 ± 0.40
NM_021099	Kit oncogene	Kit	−2.12 ± 0.10	−1.19 ± 0.20	−1.15 ± 0.18	−1.84 ± 0.11	−2.90 ± 0.07	−2.40 ± 0.10	−1.50 ± 0.13	−2.10 ± 0.10	−1.20 ± 0.18	−1.50 ± 0.12	−1.70 ± 0.12	−1.50 ± 0.17
Mitotic cell cycle														
NM_025565	SPC25, NDC80 kinetochore complex component, homolog (S. cerevisiae)	Spc25	1.79 ± 0.52	1.50 ± 0.52	−1.08 ± 0.32	2.40 ± 0.81	1.83 ± 0.57	1.34 ± 0.45	2.11 ± 0.48	1.82 ± 0.49	1.21 ± 0.32	1.66 ± 0.41	1.85 ± 0.65	1.47 ± 0.63
NM_028390	Anillin, actin binding protein	Anln	1.97 ± 0.51	1.28 ± 0.28	−1.10 ± 0.19	1.96 ± 0.48	1.60 ± 0.35	1.19 ± 0.32	1.84 ± 0.41	1.50 ± 0.33	1.18 ± 0.26	1.80 ± 0.40	1.86 ± 0.51	1.67 ± 0.41
NM_011497	Aurora kinase A	Aurka	2.31 ± 0.56	1.48 ± 0.36	1.04 ± 0.25	2.30 ± 0.55	1.46 ± 0.37	1.07 ± 0.29	1.65 ± 0.40	1.31 ± 0.32	1.11 ± 0.26	1.91 ± 0.42	1.98 ± 0.50	1.59 ± 0.44
NM_028109	TPX2, microtubule-associated protein homolog (Xenopus laevis)	Tpx2	1.80 ± 0.46	1.27 ± 0.41	−1.08 ± 0.26	1.90 ± 0.49	1.49 ± 0.45	1.06 ± 0.35	1.80 ± 0.49	1.50 ± 0.33	1.10 ± 0.25	1.70 ± 0.42	2.09 ± 0.55	1.57 ± 0.46
NM_007659	Cyclin-dependent kinase 1	Cdk1	2.58 ± 0.62	1.54 ± 0.45	−1.10 ± 0.26	3.02 ± 0.71	1.74 ± 0.38	1.18 ± 0.32	2.10 ± 0.51	1.66 ± 0.39	1.19 ± 0.26	2.06 ± 0.42	1.91 ± 0.47	1.50 ± 0.39
NM_023223	Cell division cycle 20 homolog (S. cerevisiae)	Cdc20	1.53 ± 0.50	1.06 ± 0.38	−1.15 ± 0.24	1.51 ± 0.55	1.35 ± 0.50	1.04 ± 0.46	1.87 ± 0.39	1.43 ± 0.31	−1.02 ± 0.24	1.61 ± 0.41	2.03 ± 0.50	1.32 ± 0.36
NM_013538	Cell division cycle associated 3	Cdca3	2.17 ± 0.65	1.45 ± 0.45	1.00 ± 0.28	1.94 ± 0.55	1.96 ± 0.56	1.34 ± 0.41	2.18 ± 0.62	1.78 ± 0.42	1.04 ± 0.26	1.57 ± 0.39	2.03 ± 0.48	1.43 ± 0.39
NM_172301	Cyclin B1	Ccnb1	2.75 ± 0.63	1.66 ± 0.40	1.00 ± 0.30	3.13 ± 0.82	1.85 ± 0.60	1.42 ± 0.43	2.07 ± 0.50	1.62 ± 0.41	1.19 ± 0.29	1.68 ± 0.42	2.09 ± 0.54	1.48 ± 0.51
NM_009831	Cyclin G1	Ccng1	1.30 ± 0.32	1.47 ± 0.49	1.12 ± 0.23	1.53 ± 0.47	1.35 ± 0.36	−1.01 ± 0.27	1.30 ± 0.34	1.55 ± 0.33	1.25 ± 0.34	1.36 ± 0.31	1.52 ± 0.39	1.31 ± 0.29
NM_031166	Inhibitor of DNA binding 4	Id4	1.27 ± 0.38	1.65 ± 0.48	1.07 ± 0.28	1.57 ± 0.47	2.20 ± 0.65	1.70 ± 0.59	1.36 ± 0.41	1.89 ± 0.53	1.15 ± 0.34	−1.41 ± 0.21	1.93 ± 0.56	2.11 ± 0.76
NM_010578	Integrin beta 1 (fibronectin receptor beta)	Itgb1	1.58 ± 0.33	1.29 ± 0.23	1.13 ± 0.22	1.59 ± 0.30	1.64 ± 0.31	1.13 ± 0.23	1.54 ± 0.31	1.45 ± 0.29	1.10 ± 0.20	1.34 ± 0.22	1.64 ± 0.28	1.46 ± 0.32
NM_023317	Nuclear distribution gene E homolog 1 (*A. nidulans*)	Nde1	1.40 ± 0.39	1.74 ± 0.45	1.11 ± 0.27	1.58 ± 0.42	1.89 ± 0.47	1.57 ± 0.45	1.28 ± 0.32	1.56 ± 0.35	1.24 ± 0.30	1.13 ± 0.30	1.77 ± 0.43	1.35 ± 0.35
NM_007595	Calcium/calmodulin-dependent protein kinase II, beta	Camk2b	−1.04 ± 0.16	−1.57 ± 0.13	−1.52 ± 0.11	1.00 ± 0.16	−2.10 ± 0.08	−2.30 ± 0.10	−1.31 ± 0.13	−2.47 ± 0.06	−1.71 ± 0.11	−1.18 ± 0.13	−2.33 ± 0.09	−1.74 ± 0.11
NM_008913	Protein phosphatase 3, catalytic subunit, alpha isoform	Ppp3ca	1.00 ± 0.23	−1.45 ± 0.25	−1.93 ± 0.09	1.41 ± 0.25	−1.74 ± 0.10	−2.12 ± 0.10	−1.00 ± 0.23	−2.14 ± 0.09	−1.82 ± 0.21	1.03 ± 0.20	−1.71 ± 0.11	−1.48 ± 0.12
NM_023396	Reprimo, TP53 dependent G2 arrest mediator candidate	Rprm	−1.30 ± 0.15	−1.44 ± 0.16	−1.52 ± 0.13	−1.40 ± 0.17	−1.80 ± 0.12	−1.80 ± 0.11	−1.15 ± 0.18	−1.80 ± 0.10	−1.60 ± 0.10	1.00 ± 0.18	−2.00 ± 0.09	−1.90 ± 0.11

Table 2
Genes encoding for proteins involved in mitotic cell division in individual excitotoxicity global transcriptomic profiles. Genes were selected on the basis of demonstrating at least ±1.5-fold-change expression in at least one out of three time-points (5 h, 15 h and 24 h) and passed statistical testing of one-way ANOVA, $p < 0.05$ and FDR correction. The genes were classified in the table according to the first time-point where significant regulation above or below 1.5 is detected.

300 μM AMPA	200 μM NMDA	100 μM KA	250 μM Glu
Up regulation (5 h)			
continue . . .			
• Anillin, actin binding protein	• Anillin, actin binding protein	• Anillin, actin binding protein	• Anillin, actin binding protein
• Aurora kinase A	• Aurora kinase A	• Asp (abnormal spindle)-like, microcephaly associated (Drosophila)	• Aurora kinase A
• baculoviral IAP repeat-containing 5	• Baculoviral IAP repeat-containing 5	• AT hook containing transcription factor 1	• Baculoviral IAP repeat-containing 5
• Buninhibited by benzimidazoles 1 homolog, beta (S. cerevisiae)	• Budding uninhibited by benzimidazoles 1 homolog, beta (S. cerevisiae)	• Aurora kinase A	• Cyclin B1
• Cyclin-dependent kinase 1	• Cyclin-dependent kinase 1	• Baculoviral IAP repeat-containing 5	• Cyclin-dependent kinase 1
• cell division cycle 20 homolog (S. cerevisiae)	• Cell division cycle 20 homolog (S. cerevisiae)	• Budding uninhibited by benzimidazoles 1 homolog, beta (S. cerevisiae)	• Cell division cycle associated 2
• cell division cycle associated 2	• Cell division cycle associated 2	• Cyclin-dependent kinase 1	• Cell division cycle associated 3
• cell division cycle associated 3	• Cell division cycle associated 3	• Cell division cycle 20 homolog (S. cerevisiae)	• Cell division cycle associated 5
• cell division cycle associated 5	• Cell division cycle associated 5	• Cell division cycle 6 homolog (S. cerevisiae);	• Cell division cycle associated 8
• cyclin D1	• Cell division cycle associated 8	• Cell division cycle associated 3	• E4F transcription factor 1
• cyclin D2	• Cyclin B1	• Cell division cycle associated 5	• Nucleolar and spindle associated protein 1
• DBF4 homolog (S. cerevisiae)	• Cyclin-dependent kinase 2	• Coiled-coil domain containing 99	• Polo-like kinase 1 (Drosophila)
• E4F transcription factor 1	• DBF4 homolog (S. cerevisiae)	• Cyclin D1	• Pescadillo homolog 1, containing BRCT domain (zebrafish)
• integrin beta 1 (fibronectin receptor beta)	• Integrin beta 1 (fibronectin receptor beta)	• Cyclin D2	• SPC24, NDC80 kinetochore complex component, homolog (S. cerevisiae)
• neural precursor cell expressed, developmentally down-regulated gene 9	• Kinesin family member C1	• Cyclin G1	• SPC25, NDC80 kinetochore complex component, homolog (S. cerevisiae)
• non-SMC condensin I complex, subunit H	• MAD2 mitotic arrest deficient-like 1 (yeast)	• Cyclin B1	• Sperm associated antigen 5
• polo-like kinase 1 (Drosophila)	• Microtubule-associated protein, RP/EB family, member 2	• Cyclin-dependent kinase 2	
• predicted gene 8416; predicted gene 5593; cyclin B1; similar to cyclin B1; predicted gene 4870	• Neural precursor cell expressed, developmentally down-regulated gene 1	• DBF4 homolog (S. cerevisiae)	
• regulator of chromosome condensation 2; hypothetical protein LOC100047340	• Non-SMC condensin I complex, subunit H	• E4F transcription factor 1	
	• Nucleolar and spindle associated protein 1	• Inhibitor of DNA binding 4	
	• Pituitary tumor-transforming gene 1	• Integrin beta 1 (fibronectin receptor beta)	
Up-regulation (5 h)			
• SPC25, NDC80 kinetochore complex component, homolog (S. cerevisiae)	• Polo-like kinase 1 (Drosophila)	• Microtubule-associated protein, RP/EB family, member 2	
	• SPC24, NDC80 kinetochore complex component, homolog (S. cerevisiae)	• Neural precursor cell expressed, developmentally down-regulated gene 9	
	• SPC25, NDC80 kinetochore complex component, homolog (S. cerevisiae)	• Non-SMC condensin II complex, subunit G2	
	• Sperm associated antigen 5	• Nuclear distribution gene E homolog 1 (A nidulans)	
		• Nucleolar and spindle associated protein 1	
		• ribosomal protein S6	
		• SET domain containing (lysine methyltransferase) 8	
		• Kinesin family member C1	
		• MAD2 mitotic arrest deficient-like 1 (yeast)	
		• SPC25, NDC80 kinetochore complex component, homolog (S. cerevisiae)	
		• sperm associated antigen 5	
Down-regulation at 5 h			
• NIMA (never in mitosis gene a)-related expressed kinase 3	• Calcium/calmodulin-dependent protein kinase II alpha	• CDK5 and Abl enzyme substrate 1	
		• NIMA (never in mitosis gene a)-related expressed kinase 3	
		• SAC3 domain containing 1	
		• tubulin, gamma 1	
Up-regulation at 15 h			
• Calcium/calmodulin-dependent protein kinase II, delta	• Cyclin G1	• Anaphase promoting complex subunit 1	• Cell division cycle 20 homolog (S. cerevisiae)
• Cyclin G1	• E2F transcription factor 6	• Neural precursor cell expressed, developmentally down-regulated gene 1	• Cyclin G1
• Inhibitor of DNA binding 4	• Inhibitor of DNA binding 4		• E2F transcription factor 6

• Nuclear distribution gene E homolog 1 (A nidulans) • Nucleolar and spindle associated protein 1	• MAD2 mitotic arrest deficient-like 2 (yeast) • Nuclear distribution gene E homolog 1 (A nidulans)		• Inhibitor of DNA binding 4 • Integrin beta 1 (fibronectin receptor beta) • Neural precursor cell expressed, developmentally down-regulated gene 1 • Non-SMC condensin I complex, subunit H • Nuclear distribution gene E homolog 1 (A nidulans) • Nuclear factor of activated T-cells, cytoplasmic, calcineurin-dependent 1 • Pituitary tumor-transforming gene 1
Down-regulation at 15 h • Calcium/calmodulin-dependent protein kinase II, beta • Tubulin, beta 3	• Calcium/calmodulin-dependent protein kinase II, beta • Cyclin D1 • Fibronectin type 3 and SPRY domain-containing protein • Protein phosphatase 3, catalytic subunit, alpha isoform • Ras homolog gene family, member U • Stathmin 1 • Tubulin, beta 3	• Budding uninhibited by benzimidazoles 3 homolog (S. cerevisiae) • Calcium/calmodulin-dependent protein kinase II alpha • Calcium/calmodulin-dependent protein kinase II, beta • Protein phosphatase 3, catalytic subunit, alpha isoform • Ras homolog gene family, member U • Regulator of chromosome condensation 2; hypothetical protein LOC100047340 • Calcium/calmodulin-dependent protein kinase II gamma gamma • Stathmin 1	• Amyloid beta (A4) precursor protein • Calcium/calmodulin-dependent protein kinase II alpha • Calcium/calmodulin-dependent protein kinase II, beta • Microtubule-associated protein, RP/EB family, member 2 • Polo-like kinase 2 (Drosophila) • Protein phosphatase 3, catalytic subunit, alpha isoform • Ras homolog gene family, member U
Down-regulation at 24 h • Centrin 2 • Protein phosphatase 3, catalytic subunit, alpha isoform	• Tubulin, gamma 1	• ADP-ribosylation factor-like 8A • Activating transcription factor 6 beta • Centrin 2 • Centrin 3 • Checkpoint with forkhead and ring finger domains • Chromatin modifying protein 1A; predicted gene 8515 • Thioredoxin-like 4B • Tubulin, beta 3	

Table 3
Validation of microarray data using real-time PCR technique on mouse culture treated with 250 μM Glu. Data are expressed as mean ± SE.

GenBank	Gene title	Symbol	5h		15h		24h	
			Microarray	Real-time PCR	Microarray	Real-time PCR	Microarray	Real-time PCR
NM_030704	Heat shock protein 8	Hspb8	1.29 ± 0.31	1.42 ± 0.69	4.40 ± 1.06	9.29 ± 0.55	2.63 ± 0.70	2.24 ± 0.72
NM_010442	Heme oxygenase 1	Hmox1	1.59 ± 0.34	–	2.37 ± 0.41	1.78 ± 0.62	1.51 ± 0.38	–
NM_029688	Sulfiredoxin 1 homolog	Srxn1	−1.20 ± 0.29	–	2.16 ± 0.73	2.99 ± 0.55	1.17 ± 0.43	–
NM_011121	Polo-like kinase 1	Plk1	2.08 ± 0.32	–	2.06 ± 0.37	1.64 ± 0.59	1.62 ± 0.30	–
NM_007585	Annexin A2	AnxA2	1.52 ± 0.25	–	1.93 ± 0.31	–	2.05 ± 0.43	8.25 ± 0.61
NM_020581	Angiopoietin-like 4	Angptl4	2.00 ± 0.46	3.28 ± 0.66	8.27 ± 1.62	–	8.24 ± 1.58	5.63 ± 0.58
NM_011497	Aurora kinase A	Aurka	1.91 ± 0.42	3.31 ± 0.69	1.98 ± 0.50	1.95 ± 0.72	1.59 ± 0.44	2.97 ± 1.11
NM_028109	TPX2, microtubule-associated protein homolog	Tpx2	1.70 ± 0.42	–	2.09 ± 0.55	4.79 ± 0.78	1.57 ± 0.46	4.21 ± 0.60

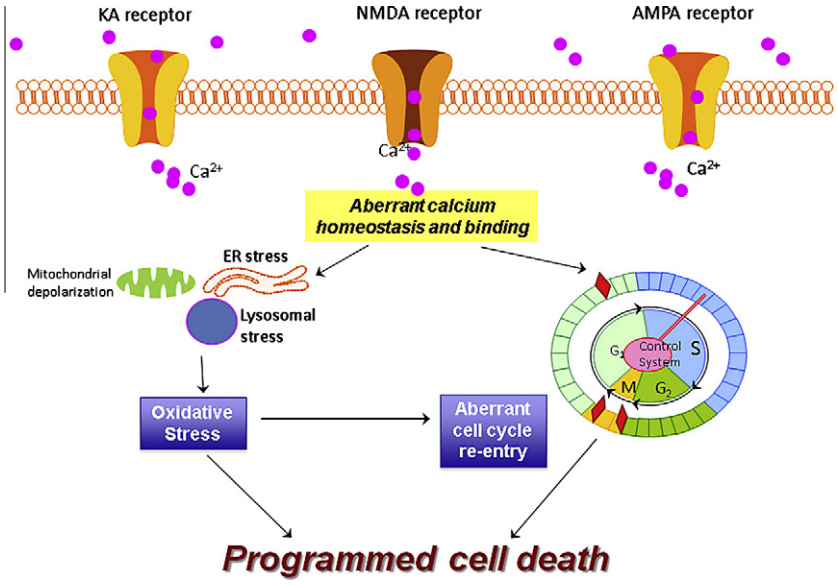

Fig. 5. A schematic diagram summarizing the proposed mechanism after over-activation of iGluR. The significant increasing of cytosolic calcium after chronic stimulation of iGluR leads to aberrant calcium homeostasis and binding. In response, ER, mitochondria and lysosome act as calcium store by uptaking the cytosolic calcium, which lead to organelle stress and subsequent oxidative stress. At the same time, both calcium influx and oxidative stress trigger cell cycle re-activation in post-mitotic neurons. Mechanistically oxidative stress and cell cycle re-entry work 'hand-in-hand' to mediate programmed cell death in excitotoxic models.

cell surfaces; (b) AMPARs are depolarized before NMDARs; (c) some AMPARs are Ca^{2+}-impermeable. In the case of Glu, delay in cellular process activation may be accounted by dilution of the effective concentration of the agonist to activate iGluRs, due to concurrent sequestration of Glu molecules by mGluRs and Glu transporters. Key findings obtained by comparison of global transcriptomic profiles were that the main pathways modulated across all excitotoxic models were calcium ion binding and homeostasis, organellar stress, oxidative stress, cell cycle re-activation and activation of cell death processes. Notably, we show for the first time that iGluR activation forms the basis of cell cycle re-activation, and that with oxidative stress they together fulfill the "two-hit" hypothesis originally formulated for AD pathogenesis (Zhu et al., 2001, 2004, 2007), suggesting that oxidative stress and cell cycle dysregulation contribute hand-in-hand to neuronal loss during neurodegeneration (Fig. 5).

Aberrant expression of neuronal cell cycle proteins with resultant neuronal loss has been observed in post-mortem tissue from patients with neurodegenerative diseases such as AD, PD, ALS, DS and progressive supranuclear palsy (Nunomura et al., 2007; Woods et al., 2007) and acute neurological disorder such as stroke and TBI (Byrnes and Faden, 2007; Timsit and Menn, 2007). Accumulating evidence has demonstrated aberrant expression of cell-cycle-related molecules in the neurons of the hippocampus, subiculum, locus coeruleus and dorsal raphe nuclei. Cell cycle re-activation association to excitotoxicity has previously been reported on numerous occasions in models of excitotoxicity and stroke, amidst models of other neurodegenerative diseases such as the MPTP model of PD and superoxide dismutase-1 mouse model of ALS (Hoglinger et al., 2007; Nguyen et al., 2003; Verdaguer et al., 2003, 2004a), indicating a similar neuropathological incidence between these two cellular events which may not be a coincidence. Based on our findings, iGluRs activation may be the origin or an important part of the cause of mitotic dysfunction.

From profiling the genes involved in mitotic cell division for individual excitotoxicity (Table 2), it is apparent that numerous cell cycle-promoting proteins were transcriptionally up-regulated from 5 h and 15 h. This finding is in agreement with an increase in gene expression of pro-mitogenic signals from growth factors. Interestingly, transcriptional up-regulation of cyclin D1 and D2 was observed in AMPA and KA models, but not in the NMDA and Glu models. This difference in temporal modulation of cyclin D could be explained by the earlier occurrence of cell cycle re-activation before the selected 5 h time-points in NMDA and Glu profile as a result of the highest physiological abundance and calcium ion

permeability of NMDARs out of the three iGluRs subtypes, which leads to the failure to capture the timeframe of cyclin D transcriptional modulation. As such, NMDA profiling demonstrated basal fold-change (~1.0) at 5 h, followed by significant pursuing down-regulation at 15 h and 24 h. On the other hand, L-cyclin D (Ccnd) transcriptional regulation was not present in the Glu profile, indicating an overall close to basal (between −1.50 and 1.50-fold) expression due to a neutralizing effect from the up and down-regulation of Ccnd in AMPA/KA and NMDA profiles, respectively upon all iGluRs activation.

While activation of iGluRs during excitotoxicity may be the trigger for the initiation of cell cycle reactivation, oxidative stress may further facilitate and promote its progression (Bonda et al., 2010). Indeed, significant oxidative load, represented by the substantial transcriptional activation of Hsps, molecular chaperones and GSH pathway associated genes, was observed across all four excitotoxicity models. Oxidative stress in particular has been strongly linked to excitotoxic neuronal cell death in both multiple sclerosis and brain ischemia (Gonsette, 2008; Warner et al., 2004). Intriguingly, our study highlights that a "two-hit" hypothesis, originally put forward for neurodegeneration in AD, involves both oxidative stress and aberrant cell cycle activation may apply to neuronal excitotoxicity (Zhu et al., 2001, 2007). In the current study, apart from oxidative stress, the two conditions paramount for aberrant cell cycle re-entry occur in neurons, namely (a) an elevation in cell cycle proteins and (b) an increase in pro-mitogenic signals, have been fulfilled. Even though mature neurons may express some cell cycle proteins, the amount produced is not sufficient to produce a substantial pro-mitogenic signal to drive the mature neuron to re-enter the cell cycle. Furthermore, some cell cycle proteins demonstrate diverse post-mitotic multi-functions that span various developmental stages of a neuron, including neuronal migration, axonal elongation, axonal pruning, dendrite morphogenesis and synaptic maturation, and plasticity (Frank and Tsai, 2009; Kim et al., 2009). As such, neuronal cell death requires the additional stimulus of pro-mitogenic molecules, such as thrombin, Aβ, ROS, nitric oxide and elevations in the level of such molecules will then trigger the mitogenic signaling cascades in injured neurons. Once mitogenic signaling is stimulated beyond a certain threshold, neurons appear to exit their quiescent state and re-enter the cell cycle and this "vulnerable" state eventually leads to their demise (Bonda et al., 2010).

To date, preclinical experiments employing inhibitors (flavopiridol, olomoucine or roscovitine) of cell cycle protein kinase family, CDKs, demonstrate improved behavioral outcomes and increased neuronal survival in a series of CNS disease models such as AD (Copani et al., 2001; Jorda et al., 2003; Verdaguer et al., 2004b), PD (Kruman and Schwartz, 2006), stroke (Osuga et al., 2000; Wang et al., 2002) and TBI (Hilton et al., 2008). All of these neuropathologies are believed to involve iGluR-mediated excitotoxicity and there is a literature suggesting inhibitors of CDKs are neuroprotective against excitotoxicity (Giardina and Beart, 2002). Overall, our gene profiling indicate that oxidative stress and cell cycle re-entry are primary events taking place during iGluR overactivation in neurons and further support the "two-hit" hypothesis for excitotoxic neuronal cell death. More importantly, our study suggests that a combined therapeutic approach using drugs that salvage oxidative stress and prevent the onset of cell cycle may potentially delay death and provide neurons with "bonus" time for recovery during excitotoxicity associated with multiple neurodegenerative diseases.

Acknowledgement

This work is supported by: NSC and PMB, project grant funding from the National Health and Medical Research Council of Australia. PMB is a Research Fellow of the NHMRC (Australia).

Appendix A. Supplementary data

Supplementary data associated with this article can be found, in the online version, at http://dx.doi.org/10.1016/j.neuint.2012.12.015.

References

Arundine, M., Tymianski, M., 2003. Molecular mechanisms of calcium-dependent neurodegeneration in excitotoxicity. Cell Calcium 34, 325–337.
Arundine, M., Tymianski, M., 2004. Molecular mechanisms of glutamate-dependent neurodegeneration in ischemia and traumatic brain injury. Cell Mol. Life Sci. 61, 657–668.
Bonda, D.J., Bajic, V.P., Spremo-Potparevic, B., Casadesus, G., Zhu, X., Smith, M.A., Lee, H.G., 2010. Review: cell cycle aberrations and neurodegeneration. Neuropathol. Appl. Neurobiol. 36, 157–163.
Byrnes, K.R., Faden, A.I., 2007. Role of cell cycle proteins in CNS injury. Neurochem. Res. 32, 1799–1807.
Camins, A., Pallas, M., Silvestre, J.S., 2008. Apoptotic mechanisms involved in neurodegenerative diseases: experimental and therapeutic approaches. Methods Find. Exp. Clin. Pharmacol. 30, 43–65.
Cheung, N.S., Carroll, F.Y., Larm, J.A., Beart, P.M., Giardina, S.F., 1998. Kainate-induced apoptosis correlates with c-Jun activation in cultured cerebellar granule cells. J. Neurosci. Res. 52, 69–82.
Cheung, N.S., Beart, P.M., Pascoe, C.J., John, C.A., Bernard, O., 2000. Human Bcl-2 protects against AMPA receptor-mediated apoptosis. J. Neurochem. 74, 1613–1620.
Copani, A., Uberti, D., Sortino, M.A., Bruno, V., Nicoletti, F., Memo, M., 2001. Activation of cell-cycle-associated proteins in neuronal death: a mandatory or dispensable path? Trends Neurosci. 24, 25–31.
Dennis Jr., G., Sherman, B.T., Hosack, D.A., Yang, J., Gao, W., Lane, H.C., Lempicki, R.A., 2003. DAVID: database for annotation, visualization, and integrated discovery. Genome Biol. 4, P3.
Doble, A., 1999. The role of excitotoxicity in neurodegenerative disease: implications for therapy. Pharmacol. Ther. 81, 163–221.
Frank, C.L., Tsai, L.H., 2009. Alternative functions of core cell cycle regulators in neuronal migration, neuronal maturation, and synaptic plasticity. Neuron 62, 312–326.
Giardina, S.F., Beart, P.M., 2002. Kainate receptor-mediated apoptosis in primary cultures of cerebellar granule cells is attenuated by mitogen-activated protein and cyclin-dependent kinase inhibitors. Br. J. Pharmacol. 135, 1733–1742.
Gonsette, R.E., 2008. Oxidative stress and excitotoxicity: a therapeutic issue in multiple sclerosis? Mult. Scler. 14, 22–34.
Graber, S., Maiti, S., Halpain, S., 2004. Cathepsin B-like proteolysis and MARCKS degradation in sublethal NMDA-induced collapse of dendritic spines. Neuropharmacology 47, 706–713.
Hara, M.R., Snyder, S.H., 2007. Cell signaling and neuronal death. Annu. Rev. Pharmacol. Toxicol. 47, 117–141.
Hilton, G.D., Stoica, B.A., Byrnes, K.R., Faden, A.I., 2008. Roscovitine reduces neuronal loss, glial activation, and neurologic deficits after brain trauma. J. Cereb. Blood Flow Metab 28, 1845–1859.
Hoglinger, G.U., Breunig, J.J., Depboylu, C., Rouaux, C., Michel, P.P., Alvarez-Fischer, D., Boutillier, A.L., Degregori, J., Oertel, W.H., Rakic, P., Hirsch, E.C., Hunot, S., 2007. The pRb/E2F cell-cycle pathway mediates cell death in Parkinson's disease. Proc. Natl. Acad. Sci. USA 104, 3585–3590.
Huang, D.W., Sherman, B.T., Lempicki, R.A., 2009. Systematic and integrative analysis of large gene lists using DAVID Bioinformatics Resources. Nat. Protoc. 4, 44–57.
Hynd, M.R., Scott, H.L., Dodd, P.R., 2004. Differential expression of *N*-methyl-D-aspartate receptor NR2 isoforms in Alzheimer's disease. J. Neurochem. 90, 913–919.
Jayakar, S.S., Dikshit, M., 2004. AMPA receptor regulation mechanisms: future target for safer neuroprotective drugs. Int. J. Neurosci. 114, 695–734.
Jorda, E.G., Verdaguer, E., Canudas, A.M., Jimenez, A., Bruna, A., Caelles, C., Bravo, R., Escubedo, E., Pubill, D., Camarasa, J., Pallas, M., Camins, A., 2003. Neuroprotective action of flavopiridol, a cyclin-dependent kinase inhibitor, in colchicine-induced apoptosis. Neuropharmacology 45, 672–683.
Kim, A.H., Puram, S.V., Bilimoria, P.M., Ikeuchi, Y., Keough, S., Wong, M., Rowitch, D., Bonni, A., 2009. A centrosomal Cdc20-APC pathway controls dendrite morphogenesis in postmitotic neurons. Cell 136, 322–336.
Kruman, I., Schwartz, E., 2006. Methods of neuroprotection by cyclin-dependent kinase inhibition. US 20080182853.
Larm, J.A., Cheung, N.S., Beart, P.M., 1997. Apoptosis induced via AMPA-selective glutamate receptors in cultured murine cortical neurons. J. Neurochem. 69, 617–622.
Lea 4th, P.M., Faden, A.I., 2003. Modulation of metabotropic glutamate receptors as potential treatment for acute and chronic neurodegenerative disorders. Drug News Perspect. 16, 513–522.
Lopes, J.P., Blurton-Jones, M., Yamasaki, T.R., Agostinho, P., LaFerla, F.M., 2009a. Activation of cell cycle proteins in transgenic mice in response to neuronal loss but not amyloid-beta and tau pathology. J. Alzheimers Dis. 16, 541–549.
Lopes, J.P., Oliveira, C.R., Agostinho, P., 2009b. Cell cycle re-entry in Alzheimer's disease: a major neuropathological characteristic? Curr. Alzheimer Res. 6, 205–212.

Mukherjee, S., Manahan-Vaughan, D., 2013. Role of metabotropic glutamate receptors in persistent forms of hippocampal plasticity and learning. Neuropharmacology 66, 65–81.

Nguyen, M.D., Boudreau, M., Kriz, J., Couillard-Despres, S., Kaplan, D.R., Julien, J.P., 2003. Cell cycle regulators in the neuronal death pathway of amyotrophic lateral sclerosis caused by mutant superoxide dismutase 1. J. Neurosci. 23, 2131–2140.

Niciu, M.J., Kelmendi, B., Sanacora, G., 2012. Overview of glutamatergic neurotransmission in the nervous system. Pharmacol. Biochem. Behav. 100, 656–664.

Nunomura, A., Moreira, P.I., Lee, H.G., Zhu, X., Castellani, R.J., Smith, M.A., Perry, G., 2007. Neuronal death and survival under oxidative stress in Alzheimer and Parkinson diseases. CNS Neurol. Disord. Drug Targets 6, 411–423.

Osuga, H., Osuga, S., Wang, F., Fetni, R., Hogan, M.J., Slack, R.S., Hakim, A.M., Ikeda, J.E., Park, D.S., 2000. Cyclin-dependent kinases as a therapeutic target for stroke. Proc. Natl. Acad. Sci. USA 97, 10254–10259.

Pelegri, C., Duran-Vilaregut, J., del Valle, J., Crespo-Biel, N., Ferrer, I., Pallas, M., Camins, A., Vilaplana, J., 2008. Cell cycle activation in striatal neurons from Huntington's disease patients and rats treated with 3-nitropropionic acid. Int. J. Dev. Neurosci. 26, 665–671.

Posner, A., Raser, K.J., Hajimohammadreza, I., Yuen, P.W., Wang, K.K., 1995. Aurintricarboxylic acid is an inhibitor of mu- and m-calpain. Biochem. Mol. Biol. Int. 36, 291–299.

Sattler, R., Tymianski, M., 2001. Molecular mechanisms of glutamate receptor-mediated excitotoxic neuronal cell death. Mol. Neurobiol. 24, 107–129.

Scheuer, K., Maras, A., Gattaz, W.F., Cairns, N., Forstl, H., Muller, W.E., 1996. Cortical NMDA receptor properties and membrane fluidity are altered in Alzheimer's disease. Dementia 7, 210–214.

Siman, R., Noszek, J.C., Kegerise, C., 1989. Calpain I activation is specifically related to excitatory amino acid induction of hippocampal damage. J. Neurosci. 9, 1579–1590.

Simpkins, K.L., Guttmann, R.P., Dong, Y., Chen, Z., Sokol, S., Neumar, R.W., Lynch, D.R., 2003. Selective activation induced cleavage of the NR2B subunit by calpain. J. Neurosci. 23, 11322–11331.

Tenneti, L., D'Emilia, D.M., Troy, C.M., Lipton, S.A., 1998. Role of caspases in *N*-methyl-D-aspartate-induced apoptosis in cerebrocortical neurons. J. Neurochem. 71, 946–959.

Timsit, S., Menn, B., 2007. Cerebral ischemia, cell cycle elements and Cdk5. Biotechnol. J. 2, 958–966.

Verdaguer, E., Jimenez, A., Canudas, A.M., Jorda, E.G., Sureda, F.X., Pallas, M., Camins, A., 2004a. Inhibition of cell cycle pathway by flavopiridol promotes survival of cerebellar granule cells after an excitotoxic treatment. J. Pharmacol. Exp. Ther. 308, 609–616.

Verdaguer, E., Jorda, E.G., Canudas, A.M., Jimenez, A., Pubill, D., Escubedo, E., Camarasa, J., Pallas, M., Camins, A., 2004b. Antiapoptotic effects of roscovitine in cerebellar granule cells deprived of serum and potassium: a cell cycle-related mechanism. Neurochem. Int. 44, 251–261.

Verdaguer, E., Jorda, E.G., Canudas, A.M., Jimenez, A., Sureda, F.X., Rimbau, V., Pubill, D., Escubedo, E., Camarasa, J., Pallas, M., Camins, A., 2003. 3-Amino thioacridone, a selective cyclin-dependent kinase 4 inhibitor, attenuates kainic acid-induced apoptosis in neurons. Neuroscience 120, 599–603.

Vincent, P., Mulle, C., 2009. Kainate receptors in epilepsy and excitotoxicity. Neuroscience 158, 309–323.

Wang, F., Corbett, D., Osuga, H., Osuga, S., Ikeda, J.E., Slack, R.S., Hogan, M.J., Hakim, A.M., Park, D.S., 2002. Inhibition of cyclin-dependent kinases improves CA1 neuronal survival and behavioral performance after global ischemia in the rat. J. Cereb. Blood Flow Metab. 22, 171–182.

Warner, D.S., Sheng, H., Batinic-Haberle, I., 2004. Oxidants, antioxidants and the ischemic brain. J. Exp. Biol. 207, 3221–3231.

Woods, J., Snape, M., Smith, M.A., 2007. The cell cycle hypothesis of Alzheimer's disease: suggestions for drug development. Biochim. Biophys. Acta 1772, 503–508.

Zhu, X., Castellani, R.J., Takeda, A., Nunomura, A., Atwood, C.S., Perry, G., Smith, M.A., 2001. Differential activation of neuronal ERK, JNK/SAPK and p38 in Alzheimer disease: the 'two hit' hypothesis. Mech. Ageing Dev. 123, 39–46.

Zhu, X., Lee, H.G., Perry, G., Smith, M.A., 2007. Alzheimer disease, the two-hit hypothesis: an update. Biochim. Biophys. Acta 1772, 494–502.

Zhu, X., Raina, A.K., Perry, G., Smith, M.A., 2004. Alzheimer's disease: the two-hit hypothesis. Lancet Neurol. 3, 219–226.